


Plasma Deposition of Solid Lubricant Coating Using AISI1020 Steel Cathode Cylinders Technique

L. L. F. Lima^{a*}, M. S. Libório^b, J. F. Medeiros Neto^c, K. S. Coan^d, L. S. Rossino^{d,e}, R. R. M. Sousa^f ,
M. G. C. B. Barbosa^f, R. M. do Nascimento^{g,h} , M. C. Feitor^a, T. H. C. Costa^a

^aUniversidade Federal do Rio Grande do Norte (UFRN), Programa de Pós-Graduação em Engenharia Mecânica, Natal, RN, Brasil.

^bUniversidade Federal do Rio Grande do Norte (UFRN), Escola de Ciência e Tecnologia (ECT), Natal, RN, Brasil.

^cUniversidade Federal do Rio Grande do Norte (UFRN), Programa de Pós-Graduação em Ciências e Engenharia de Materiais, Natal, RN, Brasil.

^dCentro Estadual de Educação Tecnológica Paula Souza (CEETEPS), Faculdade de Tecnologia do Estado de São Paulo (Fatec Sorocaba), Sorocaba, SP, Brasil.

^eUniversidade Federal de São Carlos (UFSCar), Programa de Pós-Graduação em Ciência dos Materiais, Campus Sorocaba, Sorocaba, SP, Brasil.

^fUniversidade Federal do Piauí (UFPI), Programa de Pós-Graduação em Ciências e Engenharia de Materiais, Teresina, PI, Brasil.

Received: January 03, 2023; Revised: June 13, 2023; Accepted: July 03, 2023

The use of thin films as solid lubricating makes it an excellent option for controlling wear and friction under certain operating conditions, in addition to not harming the environment. Thus, this work aims to study plasma deposition with a cathodic cage of MoS₂ thin films on AISI 1020 steel substrates. From the adaptation of the cathode Cage named cathode cylinders, the samples were treated in cathodic and floating potential with temperatures of 300 °C, 350 °C, and 400 °C in an argon atmosphere. After the treatments, they were subjected to chemical analysis by X-ray diffraction (XRD) and Raman spectroscopy, in addition to a calotest tribological test. Also, it was possible to quantify the coating thickness using scanning electron microscopy (SEM). In general, the results indicated success in the deposition of molybdenum disulfide in all samples treated at fluctuating potential, as it is possible to visualize in the XRD since it indicated the presence of peaks referring to MoS₂ and its compounds, in addition to an expressive reduction in wear through the calotest test.

Keywords: *Cathodic Cage, MoS₂, Wear.*

1. Introduction

Solid lubricants are a reality in mechanical systems used in various industry sectors¹. In recent years, this topic has been studied by several researchers who seek new materials to act as solid lubricants, new deposition methods, and improve wear resistance associated with lubricant efficiency, among other aspects¹⁻⁶.

Molybdenum disulfide has particular relevance because it is a material that has its arrangement in layers, which is essential in the wear mechanism, as it allows the sliding of its chains¹. Some researchers highlight the importance of the MoS₂ structure in the mechanism of reducing material wear and how this material has stood out in industrial applications, especially in applications involving component wear^{1,3,7-9}.

Krauß et al.⁵, Tang et al.¹⁰, Kong et al.¹¹ and Feng et al.¹² studied the effect of MoS₂ films deposited on different substrates and found that there was an increase in wear resistance of surfaces that were covered with MoS₂ films.

Libório et al.⁴ deposited MoS₂ films, by magnetron sputtering, interspersed with titanium nitride (TiN) films

to study the effect of the solid lubricating film on the wear resistance of the TiN hard film on the surface of AISI M2 steel. The authors state that MoS₂ contributes to the reduction of surface wear. Hudec et al.¹³ studied the effect of Mo-S-N lubricant film deposited on AISI M2 steel and stated that the nitrogen-doped MoS₂ film proved efficient for applications at high temperatures.

The technique of film deposition and cathodic cage nitriding is a relatively recent technique that has been applied to the deposition of different films and applications¹⁴⁻²³.

Naeem et al.^{17,23} point out that the deposition technique of thin films by cathodic cage is derived from the plasma nitriding technique by active screen, presenting the advantage in the uniformity of the deposited film, being possible to deposit films of different compositions changing only the composition of the material of the cage and the gaseous atmosphere.

However, in search of the existing literature, it was not possible to verify the deposition of materials that are not made from solid plates for making the cage²²⁻³¹.

Because it is an accessible material to deposit, the MoS₂ can be attractive to be deposited by plasma in a cathodic cage;

*e-mail: luciano.fernandes.089@ufrn.edu.br

however, as it is a commercialized material, usually in powder form, deposition using the cathodic cage technique is not feasible. Thus, in this work, we sought to develop a mechanism to facilitate the deposition of MoS_2 thin films through the cathodic cage technique. For this, a cage system was developed that uses compacted powder cylinders, originating a new technique called Cathode Cylinder Plasma Deposition (CCyPD).

2. Materials and Methods

2.1. Materials

To study the deposition of MoS_2 films, MoS_2 powders were purchased from the company FBS special lubricants, and this powder was characterized by X-Ray Diffraction, Raman Spectroscopy, and Scanning Electron Microscopy.

The substrate, AISI 1020 steel, produced by GGD Metals, was used. According to the manufacturer, the steel

follows the recommendation of international standards SAE, DIN, and UNS regarding chemical composition, having as additional elements to iron 0.17 – 0.24% C, 0.3 – 0.6% Mn, max 0.4% Si, max 0.04% P, max 0.05% S, in percent by weight. The steel samples were standardized in cylinders of 25.4 mm in diameter and 5 mm thick, prepared according to metallography standards until polished with $0.5 \mu\text{m}$ alumina and cleaned in acetone in an ultrasonic bath for 10 minutes.

For the cage, a 0.5 mm thick AISI 316 stainless steel plate was used, calendered with a final diameter of 80 mm for the cage body. As for the lid, a 3 mm thick AISI 316 stainless steel plate was used, as shown in Figure 1.

To produce cylinders MoS_2 powder was compacted under an SAE 4340 steel matrix developed, as shown in Figure 2. The matrix was dimensioned anticipating that the internal diameter of the cylinders after compaction is 8 mm, as described in the previous works^{18,23,32}.

2.2. Methods

The compaction of MoS_2 powders was carried out in a hydraulic press using a force of 1 Ton. After compaction, the cylinders were added to the cage lid and underwent a sintering process at 300°C inside the plasma reactor itself to increase their resistance. Sintering was carried out for 3 hours in an argon atmosphere in the plasma nitriding reactor, as detailed by Naeem et al.²³.

To carry out this work, we sought to vary the deposition temperature and the potential of the sample to evaluate the effect of the sample on floating potential (deposition process^{21,33} and on cathode potential (nitriding process³⁴). Thus, the treatment parameters are illustrated in Table 1.



Figure 1. Cover configuration with cylinders for deposition.

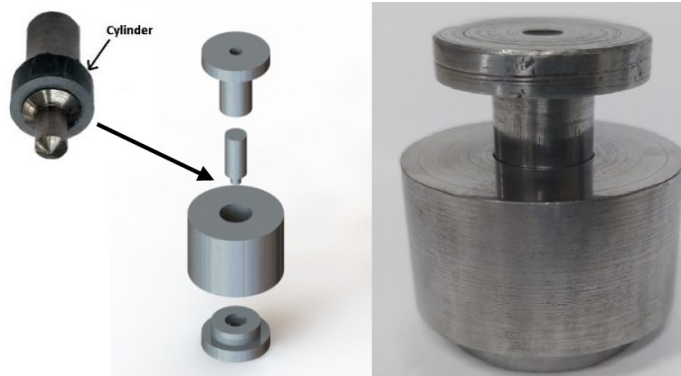


Figure 2. MoS_2 cylinder compression matrix.

Table 1. Deposition parameters with cathode cylinders.

Sample	Potential	Gas	Temperature ($^\circ\text{C}$)	Pressure (Pa)	Current (A)	Time (min)
F300	floating	Argon $15 \text{ cm}^3/\text{min}$	300	250	0.3	180
F350			350		0.45	
F400			400		0.52	
C300	cathodic		300		0.3	
C350			350		0.45	
C400			400		0.52	

After film deposition, the samples were characterized by X-ray diffraction using a Shimadzu high-resolution diffractometer (model XRD-7000) with copper $K\alpha$ radiation in the Bragg-Brentano configuration at 40 kV and 30 mA. The analysis was performed with an angle of incidence of 3° , a step of 0.02° every 0.5 s, and swept from 10° to 80° . For the layer thickness analysis, a Hitachi TM 3000 benchtop Scanning Electron Microscope was used. The composition and structural quality of the films were analyzed by Raman spectroscopy performed with the LabRAM HR Evolution system (HORIBA Scientific) with a laser of 16 mW and 633 nm. All spectra were obtained with an acquisition time of 5 s, accumulation of 10 measurements with a spectral interval of 320 - 440 cm^{-1} , observing the bands referring to the transverse acoustic (TA), longitudinal acoustic (LA), and optical transverse vibration modes (TO) resulting from first-order Raman vibrations.

The tests for the study of wear resistance were carried out in an abrasive microwear device by a fixed sphere belonging to LabTES (Laboratory of Technology and Surface Engineering) located at Fatec Sorocaba. The parameters used to carry out the tests on the base sample and with depositions were 8 N of load and 38.5 Hz of sphere rotation in which shells under shells were performed in times of 2, 5, 10, 15, 20, 25, and 30 minutes. The wear volume was calculated by Equation 1, where R corresponds to the radius of the spheres and b the diameter of the wear trails^{35,36}.

$$V = \pi \frac{b^4}{64R^2} \left(R - \frac{b^2}{8R} \right) \approx \frac{\pi b^4}{64R} \quad \text{to } b \ll R \quad (1)$$

The tests were performed without any type of abrasive or lubricant. The measurements of the trails resulting from wear were carried out using a Digital Microscope.

3. Results

Thin film deposition through the cathodic cage technique has proven efficiency in scientific studies that precede this work; as already mentioned¹⁷, the use of the sample and floating potential favors the deposition of films on the substrate and this effect can be potentiated through the gaseous atmosphere. According to Jafarpour et al.³⁷ temperature influences the thickness, morphology, and chemical composition of deposited films.

Thus, when analyzing Figure 3, where the results of the X-ray diffraction analyses are illustrated for the treated samples, in comparison with the AISI 1020 steel, it is noted that there is a difference in the intensities of the deposited phases for each configuration of treatment. Figure 3a can see the films deposited with the samples in floating potential; in this condition, according to Verbeno et al.²⁵ and Raza et al.²⁶, there is the deposition of the film without the action of a plasma on the samples, so the material torn from the cylinders is deposited at the samples under low potential difference action since the samples are at a floating potential. In this way, it is possible to verify the existence of the phases of MoS_2 and MoS_3 resulting from the pulling of these species from the cathode cylinders.

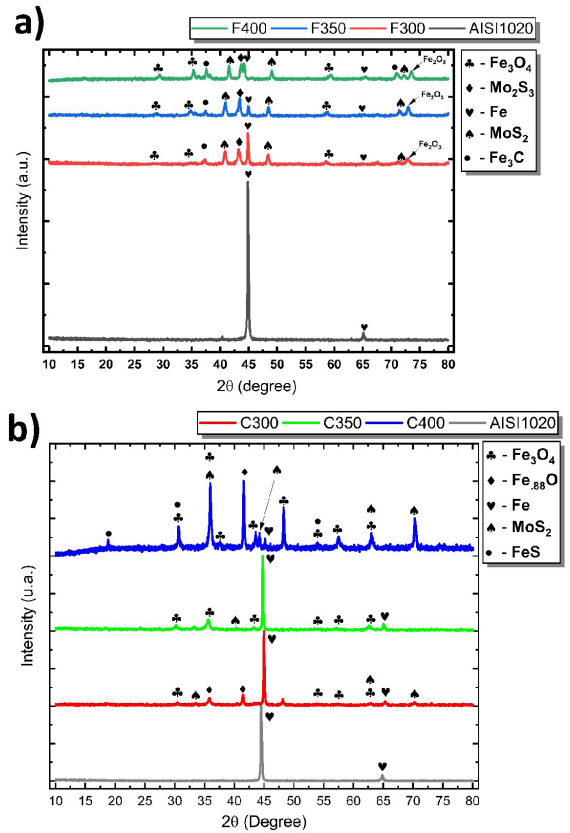


Figure 3. X-ray pattern of treated samples at a) floating and b) cathode potential.

It is also observed in Figure 3a that it is a thick film because, with the increase in temperature, the characteristic peaks of the Fe- α phases decrease in intensity. For the result illustrated in Figure 3b, it is verified that there is the deposition of MoS_2 ; however, there is a greater intensity of the oxide phases formed in samples for this treatment. The appearance of the iron oxide phases can be explained by the fact of the plasma configuration, as the samples remain at cathodic potential; that is, there is even a lower intensity presence of plasma on the samples, as described by Sumiya et al.²⁸, Coseglio et al.²⁹, and Li³⁰, sulfur acts as a decarburizing atmosphere, this fact being proven through the Fe- α peak since for the C300 and C350 samples it is possible to verify a displacement on the right, which indicates the existence of a void in the crystalline structure, caused by the removal of interstitial carbon³⁸.

Thus, in cathodic potential treatment, the samples suffer a loss of interstitial carbon species; then, the formation of oxides is more pronounced since when removing the samples from the treatment reactor, Fe oxidizes in contact with oxygen from the atmosphere.

Through the scanning electron microscopy analysis, illustrated in Figure 4, it is possible to observe that in the samples treated in cathodic potential C300 and C350, the thickness of the film is minimal, not possible to affirm the existence of a continuous film. In the C400 sample, it is noticeable the existence of a layer of compound

(white layer) in addition to the deposited thin film; this factor explains the existence of a more crystalline phase visible in Figure 3b for this sample. Nishimoto et al.³⁹ described that for treatments in plasma with a cathodic cage with the sample in cathodic potential, a simultaneous duplex treatment occurs (nitriding and deposition). For the samples treated at floating potential F300, F350, and F400, the existence of film deposition on the samples is verified. For the sample treated at 400 °C, a denser film is observed. The densification of the deposited film for the F400 sample is a factor that explains the result shown in Figure 3a since, in this way, the sample surface is completely

covered, and it is not possible to verify the peak referring to the base material (Fe- α) in the diffractogram.

Figure 5 shows the Raman spectra obtained from the surfaces of the samples where the MoS₂ deposition treatments were carried out. It is possible to observe that all the treated samples presented the vibration band in the interval 360 – 450 cm⁻¹, which is the convolution of the first-order molybdenum disulfide peaks E_{2g}¹ (~383 cm⁻¹) and A_{1g}¹ (~408 cm⁻¹). These first-order bands are due to vibrational modes within the S-Mo-S layer⁴⁰. The deconvolution of the Raman spectra was performed to obtain a more detailed view of the position and intensity of the E_{2g}¹ and A_{1g}¹ bands.

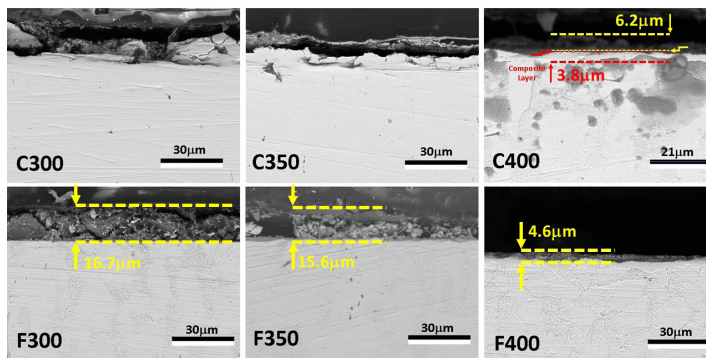


Figure 4. SEM of the cross-section of the samples with a comparison of the layer thickness deposited at cathodic and floating potential.

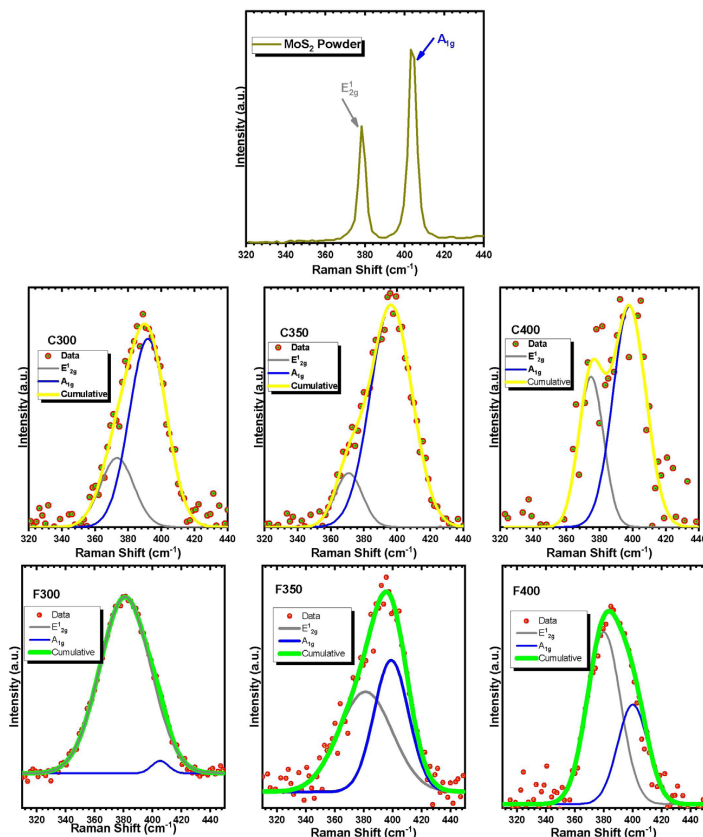


Figure 5. Raman spectroscopy with deconvolution of samples in cathodic and floating potential.

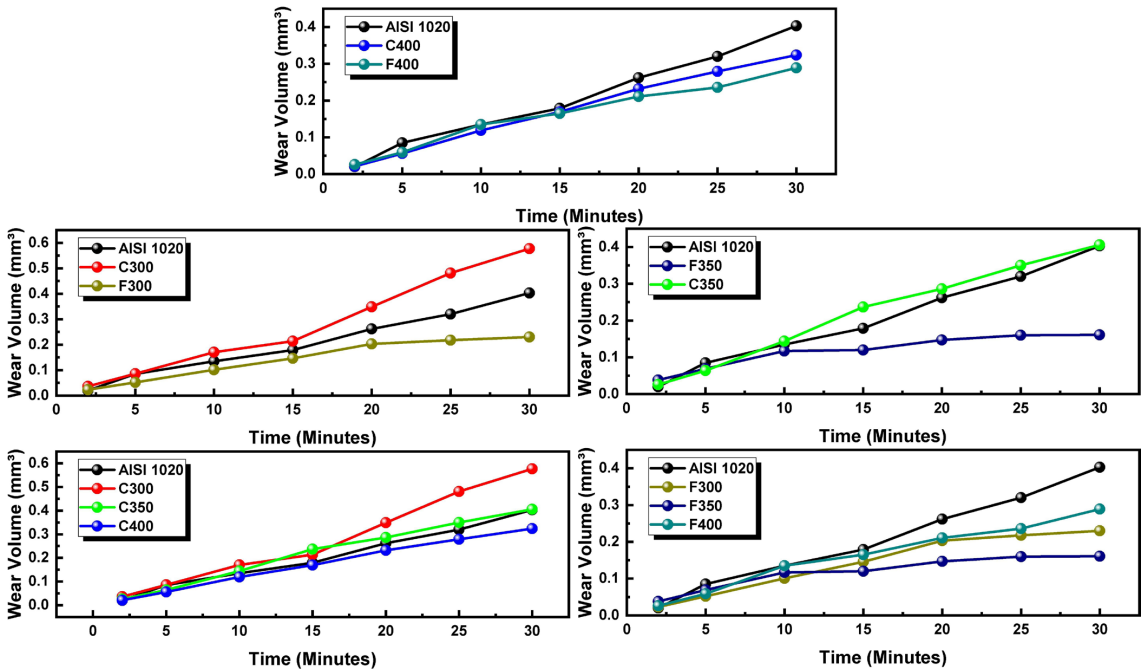


Figure 6. Wear test comparing untreated samples of AISI 1020 and treated at cathodic and floating potential.

Figure 6 shows the wear resistance of materials with and without surface treatment. It is observed that samples treated at floating potential showed more significant resistance to wear compared to samples treated at cathodic potential, with the best result to the sample treated at 350 °C, presenting a wear volume equal to 0.161 mm³, in addition, the wear volume was constant from the tenth minute of analysis.

The C300 sample showed a greater volume of wear compared to the rest of the treatments performed, whose value in the longest test time was equal to 0.577 mm³, being higher than the result obtained for the base material (0.403 mm³), which is due to the fact that the species deposited in the cathodic potential treatments come from a thermochemical treatment, that is, hard ceramic species and as seen in the SEM images, without the formation of the layer of compounds.

The C350 sample showed a more significant amount of wear in less time compared to the base material, but when it reached a time of 30 minutes, this sample showed wear values close to the base material; thus, for this sample, repetition is verified of the kinetics of the wear mechanism presented for the C300 sample, however, after some time the film is completely worn down. There is wear of the base material or the influence of a thin layer of compound that it was not possible to identify in this work.

For sample C400, due to the deposited film and the formation of the layer of compounds, there is a reduction in the wear volume and, consequently, an increase in wear resistance due to the characteristic of the film formed, as well as the deposition of MoS₂ species, as can be seen in Figure 3b.

For samples treated at a floating potential, all showed wear resistance superior to the base metal, as well as superior to samples treated at a cathodic potential. This fact proves the efficiency of the deposition of a solid lubricant film,

as well as the viability of the new cathodic cylinder plasma deposition (CCyPD).

4. Conclusion

Phases derived from MoS₂ were deposited using the cathode cylinder technique in this work. Thus, according to the results of this work, the following conclusions can be obtained:

- The XRD, SEM, and Raman spectroscopy results showed that the plasma deposition technique with cathode cylinders was efficient for the deposition of solid lubricating films originating from the sputtering effect caused in the cylinders composed of MoS₂.
- The diffractograms showed that the formation of oxides is favored when the sample is at cathode potential. This impairs the tribological behavior of plasma-treated samples compared to those treated at a fluctuating potential.
- Scanning electron microscopy results showed that more continuous films are formed in treatments at a fluctuating potential. However, the CCyPD treatment with a higher temperature (400 °C) favors the formation of a denser coating.
- The wear of the samples showed that the solid-lubricant coatings produced by the CCyPD technique with floating potential significantly reduced the surface wear volume with emphasis on the sample F350 that presented the best results.

Therefore, the technique presented in this work showed that it is possible to produce coatings similar to those obtained by cathodic cage plasma deposition. However, with the powder material compacted in the form of cylinders in which, the hollow cathode effect occurs.

5. Acknowledgments

This study was financed in part by the Coordenação de Aperfeiçoamento de Pessoal de Nível Superior - Brasil (CAPES) – Finance Code 001, and CNPq process Nº 308289/2021-8.

6. References

- Vazirisereshk MR, Martini A, Strubbe DA, Baykara MZ. Solid lubricant with MoS₂; a review. *Lubricants*. 2019;7:57.
- Verma S, Kumar V, Gupta KD. Performance analysis of flexible multirecess hydrostatic journal bearing operating with micropolar lubricant. *Lubr Sci*. 2012;24(6):273-92.
- Renevier NM, Hampshire J, Fox VC, Witts J, Allen T, Teer DG. Advantages of using self-lubricating, hard, wear-resistant MoS₂-based coatings. *Surf Coat Technol*. 2001;142-144:67-77.
- Libório MS, Praxedes GB, Lima LFF, Nascimento IG, Sousa RRM, Naeem M et al. Surface modification of M2 steel by combination of cathodic cage plasma deposition and magnetron sputtered MoS₂-TiN multilayer coatings. *Surf Coat Tech*. 2020;384:125327.
- Krauß S, Seynstahl A, Tremmel S, Meyer B, Bitzek E, Göken M et al. Structural reorientation and compaction of porous MoS₂ coatings during wear testing. *Wear*. 2022;500-501:204339.
- Al Nasser HA, Kim C, Li Q, Bissett MA, Haigh SJ, Dryfe RAW. The modified liquid | liquid interface: an electrochemical route for the electrode-less synthesis of MoS₂ metal composite thin films. *Electrochim Acta*. 2022;424:140609.
- Silva LC, Libório MS, Lima LFF, Sousa RRM, Costa THC, Naeem M et al. Deposition of MoS₂-TiN multilayer films on 1045 steel to improve common rail injection system. *J Mater Eng Perform*. 2020;29(10):6740-7.
- Zhang X, Xue Y, Ye X, Xu H, Xue M. Preparation, characterization and tribological properties of ultrathin MoS₂ nanosheets. *Mater Res Express*. 2017;4(11):115011.
- Moscoso MFC, Ramos FD, Lessa CRL, Cunha PHCP, Toniolo JC, Lemos GVB. Effects of cooling parameter and cryogenic treatment on microstructure and fracture toughness of AISI D2 tool steel. *J Mater Eng Perform*. 2020;29(12):7929-39.
- Tang G, Zhang J, Liu C, Zhang D, Wang Y, Tang H et al. Synthesis and tribological properties of flower-like MoS₂ microspheres. *Ceram Int*. 2014;40(8):11575-80.
- Kong L, Huang K, Cao X, Lu Z, Zhang G, Hu H. Effect of MoS₂ content on friction and wear properties of Mo and S co-doped CrN coatings at 25–600 °C. *Ceram Int*. 2021;47(15):21450-8.
- Feng X, Zhou H, Zheng Y, Zhang K, Zhang Y. Tribological behavior and wear mechanism of Ti/MoS₂ films deposited on plasma nitrided CF170 steel sliding against different mating materials. *Vacuum*. 2021;194:110623.
- Hudec T, Roch T, Gregor M, Orovčík L, Mikula M, Polcar T. Tribological behaviour of Mo-S-N solid lubricant coatings in vacuum, nitrogen gas and elevated temperatures. *Surf Coat Tech*. 2021;405:126722.
- Barbosa MGC, Viana BC, Santos FEP, Fernandes F, Feitor MC, Costa THC et al. Surface modification of tool steel by cathodic cage TiN deposition. *Surf Eng*. 2021;37(3):334-42.
- Araújo AGF, Naeem M, Araújo LNM, Libório MS, Danelon MR, Monção RM et al. Duplex treatment with Hastelloy cage on AISI 5160 steel cutting tools. *Mater Sci Technol*. 2022;38(8):499-506.
- Sousa FA, Costa JAP, Sousa RRM, Barbosa JCP, Araújo FO. Internal coating of pipes using the cathodic cage plasma nitriding technique. *Surf Interfaces*. 2020;21:100691.
- Naeem M, Díaz-Guillén JC, Akram M, Iqbal J, Naz MY, Shafiq M. Novel active screen plasma nitriding of aluminum using aluminum cathodic cage. *Surf Rev Lett*. 2020;27(9):1950205.
- Naeem M, Shafiq M, Zaka-ul-Islam M, Nawaz N, Díaz-Guillén JC, Zakaullah M. Effect of cathodic cage size on plasma nitriding of AISI 304 steel. *Mater Lett*. 2016;181:78-81.
- Fernades F, Rocha E Fo, Souza I, Nascimento I, Sousa R, Almeida E et al. Novel synthesis of copper oxide on fabric samples by cathodic cage plasma deposition. *Polym Adv Technol*. 2020;31(3):520-6.
- Naeem M, Zaka-ul-Islam M, Shafiq M, Bashir MI, Díaz-Guillén JC, Zakaullah M. Influence of cathodic cage diameter on mechanical properties of plasma nitrided AISI 304 steel. *Surf Coat Tech*. 2017;309:738-48.
- Sousa RRM, Araújo FO, Costa JAP, Nishimoto A, Viana BC, Alves C. Deposition of TiO₂ film on duplex stainless steel substrate using the cathodic cage plasma technique. *Mater Res*. 2016;19(5):1207-12.
- Monção RM, Araújo EA Jr, Bandeira RM, Lima CDA, Lima CL, Feitor MC et al. Evaluation of corrosion resistance of thin films formed on AISI 316L steel by plasma using hastelloy as cathodic cage. *Phys Status Solidi A*. 2021;218(10):2000578.
- Naeem M, Fortaleza VC, Serra PLC, Lima CL, Costa THC, Sousa RRM et al. Synthesis of molybdenum oxide on AISI-316 steel using cathodic cage plasma deposition at cathodic and floating potential. *Surf Coat Tech*. 2021;406:126650.
- Bashir MI, Shafiq M, Naeem M, Zaka-ul-Islam M, Díaz-Guillén JC, Lopez-Badillo CM et al. Enhanced surface properties of aluminum by PVD-TiN coating combined with cathodic cage plasma nitriding. *Surf Coat Tech*. 2017;327:59-65.
- Verbeno CH, Kröhling AC, Miranda MC, Freitas TC, Nascimento VP, Passamani EC et al. Optical, electrical, and structural properties of single-phase Ti_{2-x}N films deposited by cathodic cage. *J Vac Sci Technol B*. 2019;37(6):061214.
- Raza HA, Shafiq M, Naeem M, Naz MY, Díaz-Guillén JC, Lopez-Badillo CM. Cathodic cage plasma pre-treatment of TiN-Coated AISI-304 stainless steel for enhancement of mechanical strength and wear resistance. *J Mater Eng Perform*. 2019;28(1):20-32.
- Sousa RRM, Araújo FO, Gontijo LC, Costa JAP, Alves C Jr. Cathodic cage plasma nitriding (CCPN) of austenitic stainless steel (AISI 316): influence of the different ratios of the (N₂/H₂) on the nitrided layers properties. *Vacuum*. 2012;86(12):2048-53.
- Sumiya K, Tokuyama S, Nishimoto A, Fukui J, Nishiyama A. Application of active-screen plasma nitriding to an austenitic stainless steel small-diameter thin pipe. *Metals*. 2021;11(2):366.
- Coseglio MSDR, Li X, Dong H, Connolly BJ, Dent P, Fowler C. Corrosion behavior of active-screen plasma nitrided 17-4 PH (H1150D) steel in H₂S/CO₂-containing environments. *Corrosion*. 2019;75(10):1237-45.
- Li CX. Active screen plasma nitriding – an overview. *Surf Eng*. 2010;26(1-2):135-41.
- Li CX, Georges J, Li XY. Active screen plasma nitriding of austenitic stainless steel. *Surf Eng*. 2002;18(6):453-7.
- Sousa RRM, Araújo FO, Costa THC, Nascimento IO, Santos FEP, Alves C Jr et al. Thin tin and TiO₂ film deposition in glass samples by cathodic cage. *Mater Res*. 2015;18(2):347-52.
- Alves C, Araújo FO, Ribeiro KJB, Costa JAP, Sousa RRM, Sousa RS. Use of cathodic cage in plasma nitriding. *Surf Coat Tech*. 2006;201(6):2450-4.
- Sousa RRM, Moura YJL, Sousa PAO, Medeiros JQ No, Costa THC, Alves C Jr. Nitriding of AISI 1020 steel: comparison between conventional nitriding and nitriding with cathodic cage. *Mater Res*. 2014;17(3):708-13.
- Rutherford KL, Hutchings IM. A micro-abrasive wear test, with particular application to coated systems. *Surf Coat Tech*. 1996;79(1-3):231-9.
- Rutherford KL, Hutchings IM. Theory and application of a micro-scale abrasive wear test. *J Test Eval*. 1997;25(2):250-60.

37. Jafarpour SM, Puth A, Dalke A, Böcker J, Pipa AV, Röpcke J et al. Solid carbon active screen plasma nitrocarburizing of AISI 316L stainless steel in cold wall reactor: influence of plasma conditions. *J Mater Res Technol.* 2020;9(4):9195-205.
38. Phillips R, Jolley K, Zhou Y, Smith R. Influence of temperature and point defects on the X-ray diffraction pattern of graphite. *Carbon Trends.* 2021;5:100124.
39. Nishimoto A, Nii H, Narita R, Akamatsu K. Simultaneous duplex process of TiN coating and nitriding by active screen plasma nitriding. *Surf Coat Tech.* 2013;228(Suppl 1): S558-62.
40. Windom BC, Sawyer WG, Hahn DW. A raman spectroscopic study of MoS₂ and MoO₃; applications to tribological systems. *Tribol Lett.* 2011;42(3):301-10.